BEAM MISMATCH AND EMITTANCE OSCILLATIONS IN MAGNETIC TRANSPORT LINES

Robert J. Noble
*Fermi National Accelerator Laboratory**
Batavia, Illinois 60510

Abstract

We examine the behavior of axisymmetric space-charge dominated beams in magnetic transport lines using numerical simulation. A transport line containing two linear focusing solenoids used to match a continuous, unneutralized beam from an ion source to a radio frequency quadrupole (RFQ) is considered. We compare the beam evolution for beams with different initial emittances and density profiles. The initial emittance growth caused by nonlinear space-charge forces for a drifting beam expanding from a waist can be described by a universal curve. Subsequent emittance oscillations in the transport line result in beam mismatch at the RFQ entrance, but the effects diminish with increasing initial emittance.

Introduction

Recent progress in the understanding of emittance growth in space-charge dominated beams has provided new insight about beam evolution during transport. For these beams the space-charge term is much greater than the emittance term in the rms envelope equation (for a continuous, unaccelerated beam)

$$d^2R/dz^2 + k^2R - \epsilon^2/R^3 - K/2R = 0 \qquad (1)$$

where $R = \langle r^2\rangle^{1/2}$ is the rms beam radius, k is the focusing channel wavenumber, $\epsilon = (\langle r^2\rangle\langle v^2\rangle - \langle \vec{r}\cdot\vec{v}\rangle^2)^{1/2}$ is the rms emittance, $\vec{v} = d\vec{r}/dz$, and K is the generalized beam perveance.[1] If we define the characteristic space-charge wavenumber as $k_s = K^{1/2}/\sqrt{2}\,R$, then the condition for a space-charge dominated beam is $\epsilon/k_s R^2 \ll 1$.

The physical picture of rms emittance growth being due to the amplitude dependence of particle oscillation frequencies and the attendant filamentation of the phase space ellipse was quantified by Lapostolle.[2] He recognized that changes in space-charge field energy could be related to changes in rms emittance. More recently Anderson[3] used the fact that the internal motion of a space-charge dominated beam can be approximated by laminar flow in a cold beam ($\epsilon/k_s R^2 \to 0$) in order to calculate emittance growth. He showed that the explosive emittance growth observed in simulations[4] to occur in a quarter of a plasma period for a matched beam in a continuous focusing channel ($k = k_s$) is given by $\Delta\epsilon^2 = (U/2)k_s^2 R^4$. Here $U = \int_0^b r\,dr\,(E_s/Ne)^2 - (1 + 4\ln b/\sqrt{2}\,R)$ is the normalized space-charge field energy of the initial beam, E_s is the initial space-charge field, and the radius b is large enough to include all of the beam. For a general beam profile $U > 0$, and for a uniform profile $U = 0$.

After the first quarter of a plasma period, Anderson demonstrated that the laminar motion in a cold beam terminates abruptly with shock formation (particle velocity ceases to be a single-valued function of position). This is manifested by a local charge density spike and marks the onset of irreversible phase space dilution as space-charge potential energy is converted into thermal particle motion. In a continuous focusing channel, damped emittance oscillations follow the initial explosive emittance growth as the beam density profile oscillates between peaked and hollow distributions.

Emittance Growth in Drifting Beams

Practical transport lines for nonrelativistic ions consist of combinations of drift spaces and lenses for matching the phase space ellipse of a source beam to the acceptance of a radio frequency quadrupole (RFQ) linac. An RFQ generally requires a narrow, converging axisymmetric beam at its entrance. The parameters $\alpha = -\langle \vec{r}\cdot\vec{v}\rangle/\epsilon$ and $\beta = \langle r^2\rangle/\epsilon$ are commonly used to specify the beam envelope slope and width, respectively. Envelope integration programs such as TRACE[5] aid in the design of a beam transport line that will produce a specific α and β at an RFQ entrance. These programs assume that the beam density profile is uniform, and the rms emittance is constant.

*Operated by the Universities Research Association, Inc. under contract with the U. S. Department of Energy.

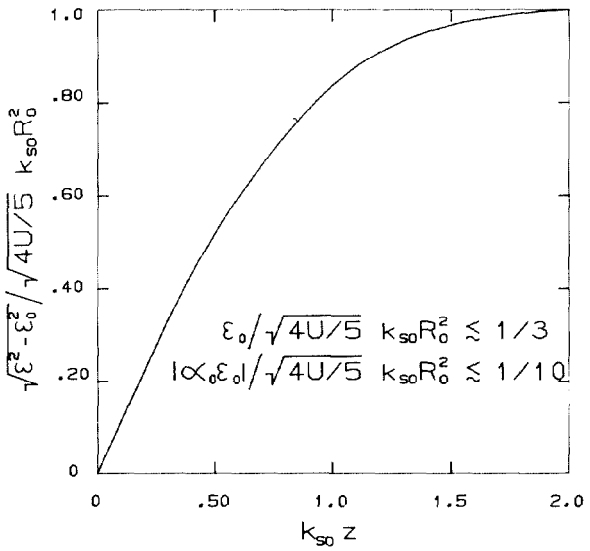

Figure 1: Universal emittance growth curve for drifting beams expanding from or near a waist.

To investigate the effect of emittance oscillations on beam matching, a special particle-in-cell (PIC) code was written in FORTRAN. The code was previously described in a study comparing the beam transport properties of magnetic solenoids and Gabor plasma lenses.[6] In that study we noted that for an unneutralized beam explosive emittance growth due to nonlinear space-charge forces occurs in the initial drift space following the ion source. Further simulations have been done using a wide variety of initial phase space distributions of the form $f(\vec{r},\vec{v}) = f_1(\vec{r})\cdot f_2(\vec{v})$ for beams expanding from or near a waist.[7] For a certain range of initial emittance ϵ_o and initial envelope slope $\alpha_o\epsilon_o$, the universal emittance growth curve in Fig. 1 was found empirically for all drifting beams when $k_{so}z < 2$. Here $k_{so} = K^{1/2}/\sqrt{2}\,R_o$ is the initial space-charge wavenumber, and R_o is the initial rms beam radius. For a beam converging (diverging) significantly at $k_{so}z = 0$, the emittance curve will lie below (above) that in Fig. 1.

For $k_{so}z > 2$ the emittance evolution for a drifting beam is somewhat dependent on the initial charge distribution, but certain general features are evident. If $\epsilon_o/\sqrt{4U/5}\,k_{so}R_o^2 < 1$, the emittance generally decreases after $k_{so}z \simeq 2$, reaches a minimum when $4 < k_{so}z < 6$ and then increases again, although more slowly than the initial explosive growth rate.[6] This emittance "bounce" becomes shallower with increasing initial emittance and disappears for $\epsilon_o/\sqrt{4U/5}\,k_{so}R_o^2 > 1$.

Mismatch in Magnetic Transport Lines

Two degrees of freedom are needed in a transport line to match a round beam's α and β to the RFQ acceptance. In a typical transport line the lens and drift lengths are not always adjustable after installation, and a minimum of two lenses is required. We will compare the beam evolution through the magnetic transport line shown in Fig. 2 for a typical range of initial emittances and different initial beam density profiles.

The lens positions and lengths shown in Fig. 2 were arbitrarily chosen symmetrically between the ion source exit and the RFQ entrance. Dimensionless parameters are used to describe the transport line in order to illustrate fundamental scalings independent of beam size and perveance. The illustrated beam envelope was obtained by integrating Eqn. (1) starting from a waist with a constant emittance $\epsilon_o/k_{so}R_o^2 = 0.1$. For space-charge dominated beams with different emittances, the beam envelopes, R/R_o, are similar

CH2669-0/89/0000-1067$01.00©1989 IEEE

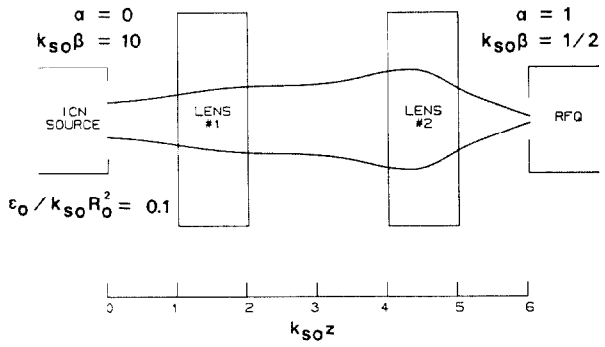

Figure 2: Magnetic transport line consisting of two solenoids showing the evolution of the rms beam envelope calculated from Eqn. 1.

except at the RFQ entrance where waist formation can be affected by both emittance and space-charge. For the three initial emittances that we will consider, the lens strengths (wavenumbers) are of course different for the same envelope match in α and $k_{so}\beta$ shown in Fig. 2:

$\varepsilon_o/k_{so}R_o^2$	k_1/k_{so}	k_2/k_{so}
0.03	0.919	1.172
0.1	0.953	1.167
0.3	0.929	1.116

As an example the initial space-charge wavenumber of a beam from a typical proton or H^- source producing several tens of mA current at a few tens of keV energy might be $k_{so} = 0.1\ cm^{-1}$ with initial mean square beam radius $R_o^2 = 0.1\ cm^2$. The source rms emittance in Figure 2 would be $\varepsilon_o = 1\ cm\ mrad$, with $\beta_{source} = 100\ cm$ and $\beta_{RFQ} = 5\ cm$. The transport line length would be 60 cm.

To illustrate the effects of different amounts of space-charge field energy on beam mismatch, we present simulation results from our PIC code for the evolution of initially parabolic (charge density $\rho \sim 1 - (r/a)^2$, $U = 0.0224$) and Gaussian ($\rho \sim exp(-r^2/\sigma^2)$, $U = 0.154$) beam density profiles through the transport line shown in Fig. 2. The results are not very sensitive to the initial divergence distribution. A Gaussian divergence distribution was used in these simulations with the initial rms emittance being $\varepsilon_o/k_{so}R_o^2 = 0.03$, 0.1 or 0.3. Gaussian distributions are truncated at two and a half times their rms size.

The emittance oscillations through the magnetic transport line are shown in Fig. 3. To illustrate any universal trends, the emittance is displayed in terms of the same function used in Fig. 1. Typically the beam profiles become nearly uniform in the first lens and then hollow in the intermediate drift space. Here some rms emittance is converted back into space-charge potential energy. The beam returns to a uniform profile after the second lens. In the final focus where the RFQ entrance would be, the emittance decreases rapidly, and the beam becomes sharply peaked with a diffuse halo. The halo contains approximately ten percent of the beam with ninety percent of the beam being within one and a half rms radii. The emittance bounce between the two lenses and the emittance reduction in the final focus are less pronounced with increasing initial emittance and space-charge field energy. This is indicative of more rapid phase-space dilution.

Figures 4 and 5 show the evolution of α and $k_{so}\beta$, respectively, in the transport line when the initial emittance is $\varepsilon_o/k_{so}R_o^2 = 0.03$. The final focus region near $k_{so}z = 6$ is magnified in Figs. 4b and 5b to illustrate the mismatch at the RFQ entrance. The mismatch in α and $k_{so}\beta$ is a combination of emittance growth and differences in rms beam radii and divergences. At $k_{so}z = 6$ the rms beam radius of the initially parabolic beam is only ten percent greater than the envelope prediction ($\langle r^2\rangle^{1/2}/R_o = 0.123$) while that of the Gaussian is more than twice as great. This is partially due to the beam halos which for the parabolic beam extends to about three rms beam radii and for the Gaussian beam to about six rms radii.

Figures 6 and 7 show the evolution of α and $k_{so}\beta$, respectively, in the transport line when the initial emittance is $\varepsilon_o/k_{so}R_o^2 = 0.3$. The intermediate case for an initial emittance $\varepsilon_o/k_{so}R_o^2 = 0.1$ was illustrated in Ref. 6 and is not reproduced here. The trend however is clearly toward less mismatch with increasing initial emittance since space-charge field energy contributes proportionally less to emittance growth. Interestingly, halo formation is also reduced with increasing initial emittance. At $k_{so}z = 6$ the rms radius of the parabolic beam is nearly equal to the envelope prediction ($\langle r^2\rangle^{1/2}/R_o = 0.39$) while that of the Gaussian is only six percent greater for the case illustrated in Figs. 6 and 7. The beam halos for the parabolic and Gaussian beams extend to about two and three rms radii, respectively.

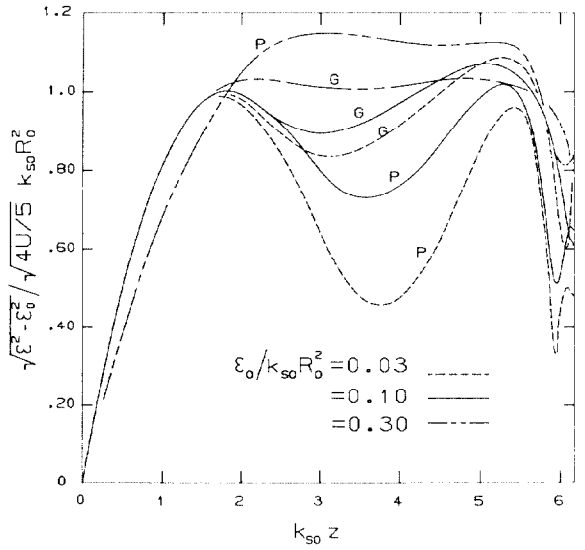

Figure 3: Emittance oscillations for initially parabolic (P) and Gaussian (G) beams with different initial emittances in a transport line containing two magnetic solenoids.

Conclusion

In a transport line containing two magnetic solenoids, emittance oscillations of an unneutralized beam generally involve an emittance bounce between the two solenoids and an emittance reduction in the final focus. The emittance bounce and final focus reduction become less pronounced with increasing initial emittance and space-charge field energy indicating more rapid dilution. The explosive emittance growth in the initial drift due to nonlinear space-charge forces follows a universal curve for a certain range of initial emittance and initial envelope slope. Beam mismatch in the final focus (when compared with simple envelope integration) is reduced with increasing initial emittance and decreasing space-charge field energy.

References

1. J.D. Lawson, "Space Charge Optics," Adv. Electronics and Electron Phys., Suppl. 13C, 1 (1980). The perveance $K = 2N r_c/\beta_r^2\gamma_r^3$, where N is the number of beam particles per unit length, r_c is the classical particle radius, and β_r and γ_r are the usual relativistic quantities. The perveance is essentially the ratio of a particle's space-charge potential energy at the beam center relative to the beam edge and longitudinal kinetic energy.

2. P.M. Lapostolle, "Possible Emittance Increase through Filamentation Due to Space Charge in Continuous Beams," IEEE Trans. Nucl. Sci., Vol. 18, 1101 (1971).

3. O.A. Anderson, "Internal Dynamics and Emittance Growth in Space-Charge Dominated Beams," Particle Accelerators, Vol. 21, 197 (1987).

4. T.P. Wangler, K.R. Crandall, R.S. Mills and M. Reiser, "Relation Between Field Energy and RMS Emittance in Intense Particle Beams," IEEE Trans. Nucl. Sci., Vol. 32, 2196 (1985).

5. K.R. Crandall and D.P. Rusthoi, "Documentation for TRACE: An Interactive Beam-Transport Code," Los Alamos Report LA-10235-MS (January 1985).

6. R.J. Noble, "Beam Transport with Magnetic Solenoids and Plasma Lenses," presented at the 1988 Linear Accelerator Conference, Williamsburg, Virginia, October 3-7, 1988.

7. An initially expanding or contracting beam is simulated by giving each macroparticle an added initial transverse velocity proportional to its radial position (ballistic focusing). The corresponding initial tilt of the phase space ellipse is $\alpha_o\varepsilon_o/k_{so}R_o^2 = -\langle \vec{r}\cdot\vec{v}\rangle_o/k_{so}R_o^2 = 1/k_{so}z_b$, where k_{so} is the initial space-charge wavenumber, and z_b is the ballistic focal length.

8. The initial emittance growth rate for a drifting beam has been calculated by E.P. Lee, S.S. Yu and W.A. Barletta, "Phase-Space Distortion of a Heavy-Ion Beam Propagating through a Vacuum Reactor Vessel," Nucl. Fusion, Vol. 21, 961 (1981)).

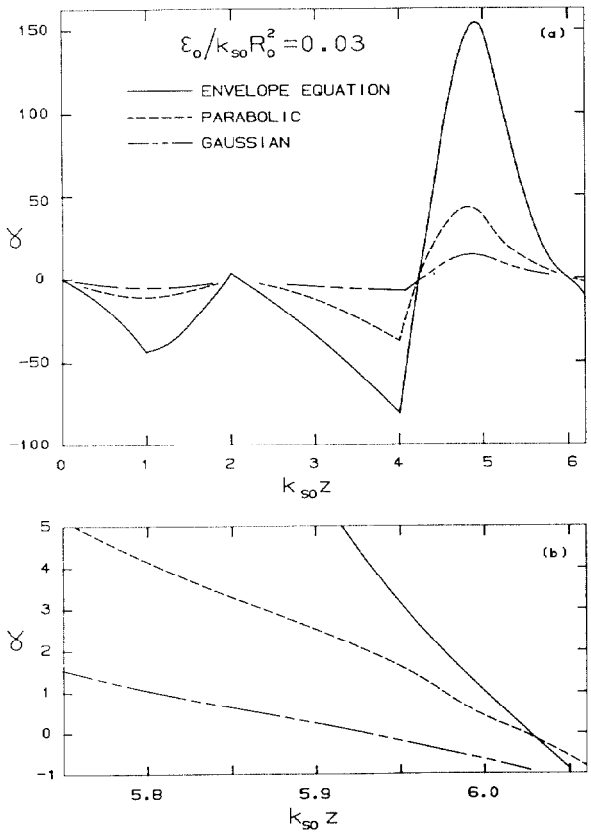

Figure 4: Evolution of α (a) through the transport line containing two magnetic solenoids and (b) in the final focus region near $k_{so}z = 6$ when the initial emittance is $\varepsilon_o/k_{so}R_o^2 = 0.03$.

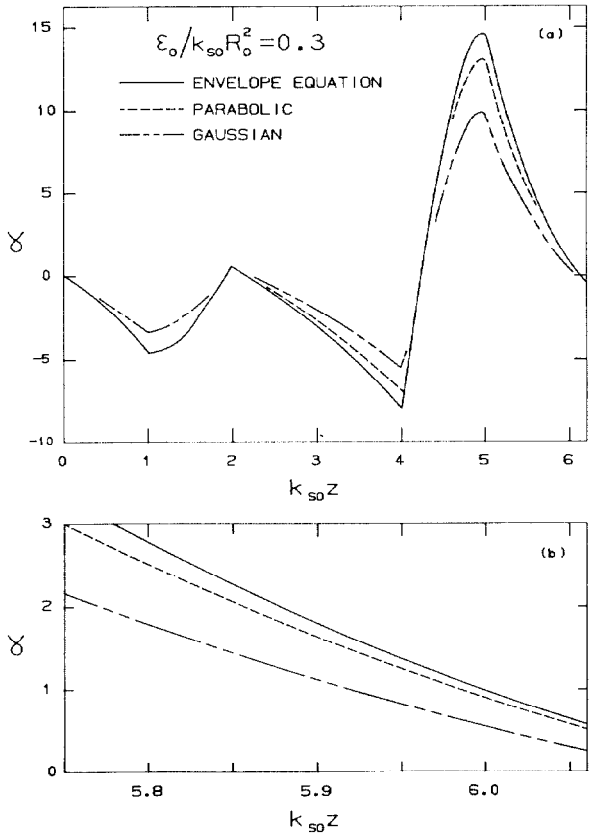

Figure 6: Evolution of α (a) through the transport line containing two magnetic solenoids and (b) in the final focus region near $k_{so}z = 6$ when the initial emittance is $\varepsilon_o/k_{so}R_o^2 = 0.3$.

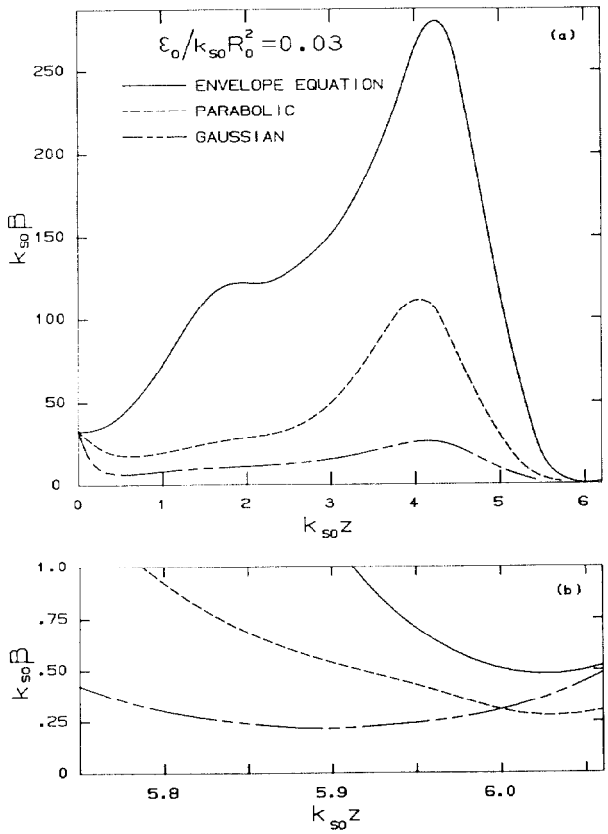

Figure 5: Evolution of $k_{so}\beta$ (a) through the transport line containing two magnetic solenoids and (b) in the final focus region near $k_{so}z = 6$ when the initial emittance is $\varepsilon_o/k_{so}R_o^2 = 0.03$.

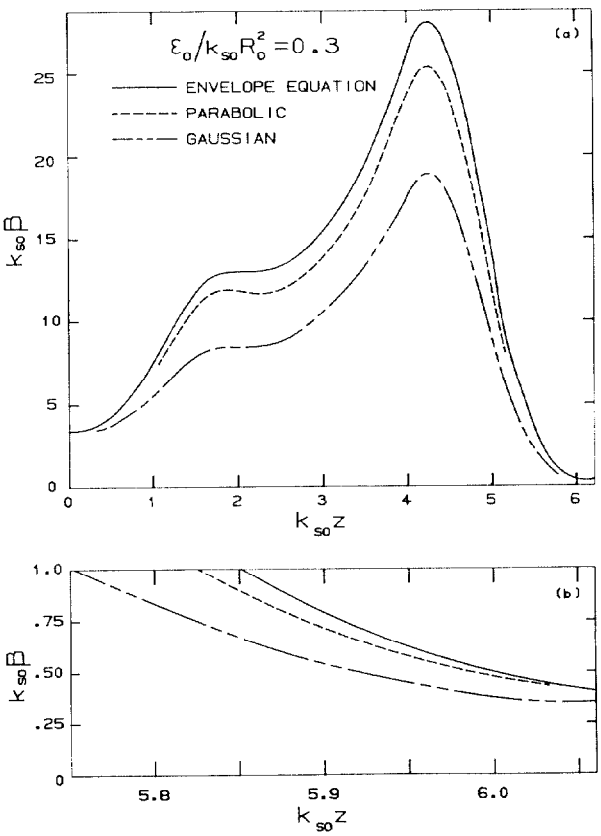

Figure 7: Evolution of $k_{so}\beta$ (a) through the transport line containing two magnetic solenoids and (b) in the final focus region near $k_{so}z = 6$ when the initial emittance is $\varepsilon_o/k_{so}R_o^2 = 0.3$.